# Computer Simulation Studies of the Catalytic Mechanism of Human Aldose Reductase

**Péter Várnai[†] and Arieh Warshel*[,‡]**

*Contribution from the Physical and Theoretical Chemistry Laboratory, Oxford University, South Parks Road, Oxford OX1 3QZ, United Kingdom, and Department of Chemistry, University of Southern California, Los Angeles, California 90089-1062*

*Received December 6, 1999*

**Abstract:** Aldose reductase, an NADPH dependent oxidoreductase, has received considerable attention due to its possible link to diabetic and galactosemic complications. It is known that the catalytic reaction involves a hydride shift from NADPH and a proton transfer from a suitable proton donor to the carbonyl group of the substrate. However, the details of the process are still unclear. The present work explores the catalytic mechanism of the enzyme by using the semi-microscopic protein dipoles Langevin dipoles (PDLD/S) and the empirical valence bond (EVB) methods. The p$K_a$ values of His-110 and Tyr-48 are evaluated to determine which of these two residues donates the proton in the reaction. It is found that the free energy of protonation of His-110 in its protein site is ∼9 kcal/mol and hence the p$K_a$ of this residue is abnormally low. Consequently, His-110 is not protonated in the active site of aldose reductase. On the other hand, it is found that the p$K_a$ of Tyr-48 is lowered to ∼8.5 in the active site due to the stabilization by the unique local environment of the phenol group. We conclude that Tyr-48 acts as the proton donor in the reduction of aldehydes by aldose reductase, while the neutral His-110 has a role in substrate binding during the catalysis. To obtain a quantitative picture of the energetics of different feasible catalytic mechanisms in the protein we follow the EVB philosophy and calibrate the potential surface of the catalytic reaction in a solvent cage by using the relevant energetics from experiments. It is found that a mechanism where a proton transfer precedes the hydride transfer is unfavorable in the solvent cage, relative to the alternative mechanism where the hydride transfer precedes protonation. Furthermore, our study of the reaction in the actual protein environment indicates that an initial proton transfer step would require prohibitively high energy. Thus, the most probable catalytic mechanism commences with the hydride shift, followed by a proton transfer from Tyr-48. The calculations show that in water the activation barrier for the hydride shift is ∼20 kcal/mol, which is far above the barrier of the subsequent proton transfer. The protein environment stabilizes the transition state of the hydride shift by ∼3 kcal/mol and destabilizes the intermediate state by ∼8 kcal/mol relative to the corresponding states in the water cage. This finding is consistent with the physiological role of the enzyme in detoxification where it catalyzes the reduction of a wide range of carbonyl-containing substrates without particular specificity. It is argued that it may be difficult for an enzyme to both satisfy this demand and catalyze the reaction beyond the simple role of bringing the proton and hydride donor groups to the proximity of the substrate.

## 1. Introduction

Human aldose reductase (ALR2, EC 1.1.1.21), a member of the aldo-keto oxidoreductase superfamily,[1] catalyzes the reduction of a variety of carbonyl compounds to the corresponding alcohols. The enzyme is a monomer (35.8 kDa) encoded by a single gene located on chromosome region 7q35.[2,3] It is expressed in various human tissues including retina,[4] muscle,[4] placenta,[1] and liver.[5] The enzyme utilizes NADPH cofactor to reduce carbonyl compounds such as sugars,[6] corticosteroid hormones[7] and aldehyde metabolites.[1,8] The physiological role of ALR2 spans from steroid and carbohydrate metabolism[9] to detoxification.[10,11] The enzyme has received considerable attention due to its participation in the polyol pathway where it reduces glucose and galactose under hyperglycemic conditions.[12] The excessive accumulation of the products of these enzymatic reactions is believed to be linked to certain long-term diabetic and galactosemic complications such as cataract, retinopathy, nephropathy, and neuropathy.[12,13] Interruption of the polyol

* Corresponding author. Telephone: +1-213-740-4114. Fax: +1−213-740-2701. E-mail: warshel@invitro.usc.edu.

[†] Oxford University

[‡] University of Southern California.

(1) Bohren, K. M.; Bullock, B.; Wermuth, B.; Gabbay, K. H. *J. Biol. Chem.* **1989**, *264*, 9547−9551.

(2) Graham, A.; Brown, L.; Hedge, P. J.; Gammack A, J.; Markham, A. F. *J. Biol. Chem.* **1991**, *266*, 6872−6877.

(3) Graham, A.; Heath, P.; Morten, J. E.; Markham, A. F. *Hum. Genet.* **1991**, *86*, 509−514.

(4) Nishimura, C.; Matsuura, Y.; Kokai, Y.; Akera, T.; Carper, D.; Morjana, N.; Lyons, C.; Flynn, T. G. *J. Biol. Chem.* **1990**, *265*, 9788−9792.

(5) Graham, A.; Hedge, P. J.; Powel, S. J.; Riley, J.; Brown, L.; Gammack, A.; Carey, F.; Markham, A. F. *Nucleic Acids Res.* **1989**, *17*, 8368.

(6) Hers, H. G. *Biochim. Biophys. Acta* **1956**, *22*, 202−203.

(7) Wermuth, B.; Monder, C. *Eur. J. Biochem.* **1983**, *131*, 423−426.

(8) Vander Jagt, D. L.; Robinson, B.; Taylor, K. K.; Hunsaker, L. A. *J. Biol. Chem.* **1992**, *267*, 4364−4369.

(9) Warren, J. C.; Murdock, G. L.; Ma, Y.; Goodman, S. R.; Zimmer, W. E. *Biochemistry* **1993**, *32*, 1401−1406.

(10) Grimshaw, C. E. *Biochemistry* **1992**, *31*, 10139−10145.

(11) Vander Jagt, D. L.; Kolb, N. S.; Vander Jagt, T. J.; Chino, J.; Martinez, F. J.; Hunsaker, L. A.; Royer, R. E. *Biochim. Biophys. Acta* **1995**, *1249*, 117−126.

(12) Kador, P. F. *Med. Res. Rev.* **1988**, *8*, 325−352.

10.1021/ja994246j CCC: $19.00 
Published on Web 04/08/2000

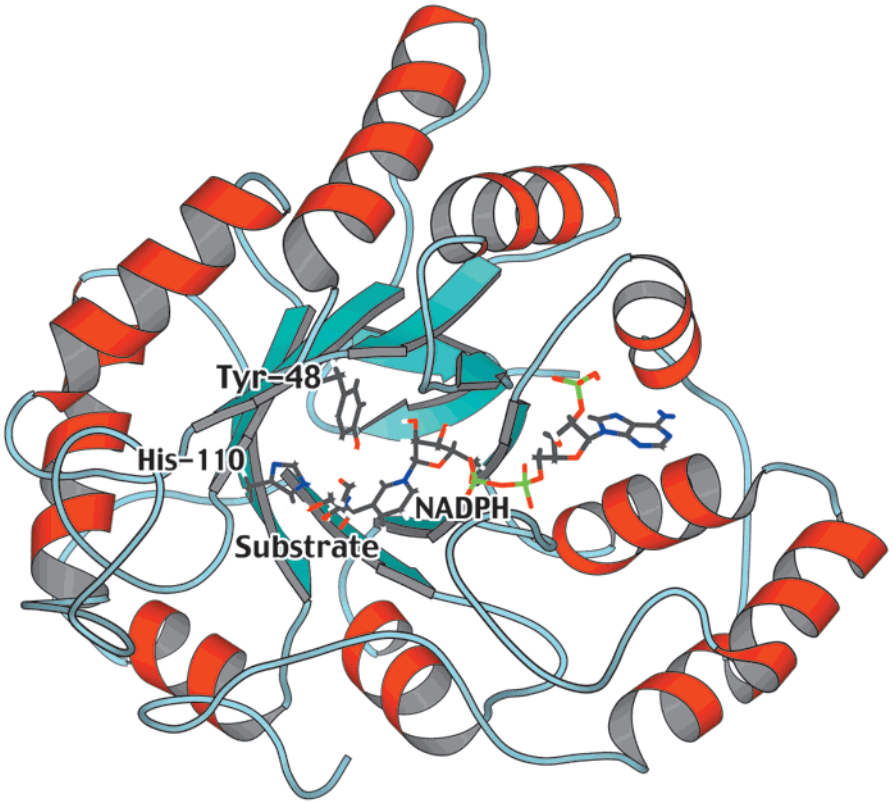


**Figure 1.** Perspective view[19] of the structure of human aldose reductase with bound NADPH. The cofactor and some important residues which are considered in the text are shown in a stick representation.

pathway with the administration of aldose reductase inhibitors (ARIs) represents a potential therapeutic strategy for preventing the onset or progression of these complications.[14] At present, the available drugs are not effective due to their side effects and nonspecificity. To develop a rational basis for the design of new, specific ARIs, it is necessary to understand the mechanism of the catalytic reaction on a detailed molecular level.

Several crystal structures have been determined for the apoenzyme,[15] the holoenzyme, and the inhibitor-bound holoenzyme[16−18] (Figure 1), as well as for mutant enzymes.[20−22] Structural analysis and kinetic experiments have revealed important aspects of the enzymatic reaction mechanism. It has been shown[23,24] that the enzymatic reaction is initiated when the NADPH cofactor binds to the apoenzyme. This is followed by the binding of the substrate and the catalytic reaction. Finally, the substrate is released, and the oxidized cofactor $NADP^+$ dissociates from the complex. The binding and release of the cofactor is associated with a conformational change in the enzyme that is the major rate-limiting factor in the overall reaction. It has been established[16] that the large and highly hydrophobic active site is located at the carboxyl terminus of the $(\beta/\alpha)_8$ barrel. In the catalytic reaction, the *pro-R* hydrogen of the NADPH is transferred to the *re* face of the carbonyl group of the substrate,[25] followed or preceded by a protonation of the carbonyl oxygen of the substrate by a suitable proton donor in its vicinity (Figure 2).

There are two potential proton donor residues in the active site of ALR2, which are conserved in the aldo−keto oxidoreductase superfamily: Tyr-48 and His-110. Histidines often serve as proton donors in biological systems[26] due to the fact that their $pK_a$ is approximately 6.5 in aqueous solution. In the case of ALR2, however, mutations of His-110 to Asn,[27] Gln, or Ala[21] exhibited reduced but measurable enzymatic activities. The hydrophobic environment[16,21] of His-110 and the existence of a conserved water channel that connects N$\delta$1 of His-110 to the bulk solvent[28,29] led to controversial conclusions about the protonation state of this residue. A study of the pH dependence of steady-state kinetic parameters suggested[30] that His-110 is

(13) Gabbay, K. H. *N. Engl. J. Med.* **1973**, *288*, 831−836.
(14) Sarges, R.; Oates, P. *Prog. Drug Res.* **1993**, *40*, 99−161.
(15) Rondeau, J.-M.; Tête-Favier, F.; Podjarny, A.; Reymann, J.-M.; Barth, P.; Biellmann, J.-F.; Moras, D. *Nature* **1992**, *355*, 469−472.
(16) Wilson, D. K.; Bohren, K. M.; Gabbay, K. H.; Quiocho, F. A. *Science* **1992**, *257*, 81−84.
(17) Wilson, D. K.; Tarle, I.; Petrash, J. M.; Quiocho, F. A. *Proc. Natl. Acad. Sci. U.S.A.* **1993**, *90*, 9847−9851.
(18) Harrison, D. H.; Bohren, K. M.; Ringe, D.; Petsko, G. A.; Gabbay, K. H. *Biochemistry* **1994**, *33*, 2011−2020.
(19) Kraulis, P. J. *J. Appl. Crystallogr.* **1991**, *24*, 946−950.
(20) Bohrani, D. W.; Harter, T. M.; Petrash, J. M. *J. Biol. Chem.* **1992**, *267*, 24841−24847.
(21) Bohren, K. M.; Grimshaw, C. E.; Lai, C. J.; Harrison, D. H.; Ringe, D.; Petsko, G. A.; Gabbay, K. H. *Biochemistry* **1994**, *33*, 2021−2032.
(22) Urzhumtsev, A.; Tête-Favier, F.; Mitschler, A.; Barbanton, J.; Barth, P.; Urzhumtseva, L.; Biellmann, J.-F.; Podjarny, A. D.; Moras, D. *Structure* **1997**, *5*, 601−612.
(23) Grimshaw, C. E.; Shahbaz, M.; Putney, C. G. *Biochemistry* **1990**, *29*, 9947−9955.
(24) Kubieski, T. J.; Hyndman, D. J.; Morjana, N. A.; Flynn, T. G. *J. Biol. Chem.* **1992**, *267*, 6510−6517.
(25) Feldman, H. B.; Szczepanik, P. A.; Havre, P.; Corrall, R. J. M.; Yu, L. C.; Rodman, H. M.; Rosner, B. A.; Klein, P. D.; Landau, B. R. *Biochim. Biophys. Acta* **1977**, *480*, 14−20.
(26) Fersht, A. *Structure and mechanism in protein science*; W. H. Freeman & Co.: New York, 1999.
(27) Tarle, I.; Borhani, D. W.; Wilson, D. K.; Quiocho, F. A.; Petrash, J. M. *J. Biol. Chem.* **1993**, *268*, 25687−25693.
(28) Tête-Favier, F.; Barth, P.; Mitchler, A.; Podjarny, A. D.; Rondeau, J. M.; Urzhumtsev, A.; Biellmann, J.-F.; Moras, D. *Eur. J. Med. Chem.* **1995**, *30 S*, 589−603.
(29) Lee, Y. S.; Hodoscek, M.; Brooks, B. R.; Kador, P. F. *Biophys. Chem.* **1998**, *70*, 203-216.
(30) Liu, S. Q.; Bhatnagar, A.; Srivastava, S. K. *J. Biol. Chem.* **1993**, *268*, 25494−25499.

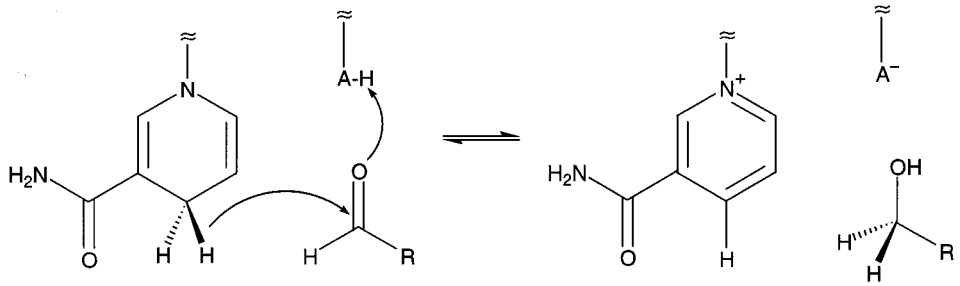


**Figure 2.** Schematic description of the catalytic reaction of aldose reductase. The reduction involves a stereospecific hydride transfer from the nicotinamide ring of NADPH to the substrate carbonyl carbon and a protonation from a suitable proton donor (AH) to the substrate carbonyl oxygen.

protonated and probably the catalytic proton donor. Alternatively, Tyr-48 was proposed to be the proton donor on the basis of structural analysis.[16] The p$K_a$ value for tyrosine in aqueous solution of ~10 is believed to be lowered to 8.25 in the conserved Tyr-48-Lys-77-Asp-43 triad in the active site of ALR2.[31] Site-directed mutagenesis studies also support a mechanism in which Tyr-48 is the proton donor. No catalytic activity was detectable in the Tyr-48→Phe (Y48F)[21] and Lys-77→Met (K77M) mutants,[21] and reduced catalytic activity was observed in the Asp-43→Asn (D43N) mutant.[27] However, some activity was retained in the mutants where Tyr-48 was replaced by His (Y48H) and Ser (Y48S).[21] To explain this observation, it was suggested that the proton donor is the water molecule which is found in the crystal structure of the Y48H mutant at the location corresponding to that of the Tyr-48 hydroxyl group in the wild-type crystal structure.[21]

Despite the experimental evidence that Tyr-48 is the likely proton donor in the native enzyme it has been found in recent computer simulation studies[29,32] that the activation barrier is lower when the protonated form of His-110 acts as the proton donor as opposed to Tyr-48. However, these calculations overlooked the fact that His-110 may not be protonated in the hydrophobic protein environment. A rather qualitative molecular modeling study[33] proposed a neutral His-110 in the ternary complex on the basis of calculated binding geometries and interaction enthalpies. It should be noted in this respect that calculations of structures of proteins in different charged configurations are very problematic without the proper treatment of long-range effects and, more importantly, ionization states should be determined by energy calculations of the protein in its charged and uncharged states rather than by structural calculations. Despite the possible problems with the above theoretical studies it is clear that computer simulation approaches are essential to correlate the structure and function of proteins, and this should also be true for ALR2. Such studies can provide, at least in principle, information about the relative energies of different reaction paths and thus the feasibility of alternative mechanisms. In the present work we use computer simulation approaches to obtain more reliable results by evaluating the p$K_a$ values of His-110 and Tyr-48 and the energetics of other relevant charge configurations. Further, we analyze the energetics of different feasible mechanisms of the catalytic reaction in a solvent cage on the basis of experimental free energy data. This allows us to explore the catalytic effect of the enzyme by considering the difference between the free energy of different mechanisms in solution and in the actual protein environment. The calculated results and their relevance to the available experimental data are discussed, and the possible connection between our findings and the role of the enzyme in physiological detoxification is considered.

## 2. Methods

**2.1. p$K_a$ Calculations.** The dissociation energy of chemical bonds depends on the surrounding environment. For example, while the dissociation of an acid is thermodynamically unfavorable in the gas phase, it proceeds spontaneously in aqueous solution. The medium in the interior of biological macromolecules is highly complex and can significantly stabilize or destabilize the ionized group. Therefore, it is important to calculate the free-energy change of the dissociation process (or the corresponding p$K_a$) by using a proper description of the electrostatic interactions between the ionizable group and its surroundings.[34−37] Although it is possible to calculate the absolute p$K_a$ value of an ionizable group, more accurate results can be obtained by evaluating the difference in free energy of solvation upon changing the environment of the given group from water to the active site of the enzyme.[34−36,38] The free energy associated with the p$K_a$ of an ionizable group (AH) can be calculated by using the central thermodynamic cycle of Figure 3.[34]

$$\Delta G^{p}(AH_p \rightarrow A_p^- + H_w^+) = \Delta G^{w}(AH_w \rightarrow A_w^- + H_w^+) + \Delta G_{sol}^{w\rightarrow p}(A^-) - \Delta G_{sol}^{w\rightarrow p}(AH) \quad (1)$$

where p and w denote the protein and water environment for the dissociation process, respectively, and $\Delta G_{sol}^{w\rightarrow p}$ is the difference in free energy of solvation upon moving the indicated group from water to its protein site. Equation 1 can be rewritten as

$$pK_{a,i}^{p} = pK_{a,i}^{w} + \frac{1}{2.3RT}\Delta\Delta G_{sol}^{w\rightarrow p}(AH_i \rightarrow A_i^-) \quad (2)$$

where $pK_{a,i}^{p}$ and $pK_{a,i}^{w}$ are the p$K_a$'s of the $i$th group in protein and water, respectively, and $\Delta\Delta G_{sol}^{w\rightarrow p}$ ($AH_i \rightarrow A_i^-$) consists of the last two terms of eq 1. Since $pK_{a,i}^{w}$ can be determined experimentally to a high degree of accuracy, one needs to focus only on the second term in eq 2.

$\Delta\Delta G_{sol}^{w\rightarrow p}$ for $A^-$ or AH can be obtained with the semi-microscopic protein dipoles Langevin dipoles (PDLD/S) method[39,40] coupled with

(31) Grimshaw, C. E.; Bohren, K. M.; Lai, C., -J.; Gabbay, K. H. *Biochemistry* **1995**, *34*, 14374−14384.
(32) Várnai, P.; Richards, W. G.; Lyne, P. D. *Proteins: Struct., Funct., Genet.* **1999**, *37*, 218−227.
(33) De Winter, H. L.; von Itzstein, M. *Biochemistry* **1995**, *34*, 8299−8308.
(34) Warshel, A. *Biochemistry* **1981**, *20*, 3167−3177.
(35) Russel, S. T.; Warshel, A. *J. Mol. Biol.* **1985**, *185*, 389−404.
(36) Sharp, K. A.; Honig, B. *Annu. Rev. Biophys. Chem.* **1990**, *19*, 301−332.
(37) Warshel, A. *J. Biol. Chem.* **1998**, *273*, 27035−27038.
(38) Warshel, A. *Computer Modeling of Chemical Reactions in Enzymes and Solutions*; John Wiley & Sons: New York, 1991.
(39) Warshel, A.; Náray-Szabó, G.; Sussman, F.; Hwang, J.-K. *Biochemistry* **1989**, *28*, 3629−3637.
(40) Lee, F. S.; Chu, Z. T.; Warshel, A. *J. Comput. Chem.* **1993**, *14*, 161−185.

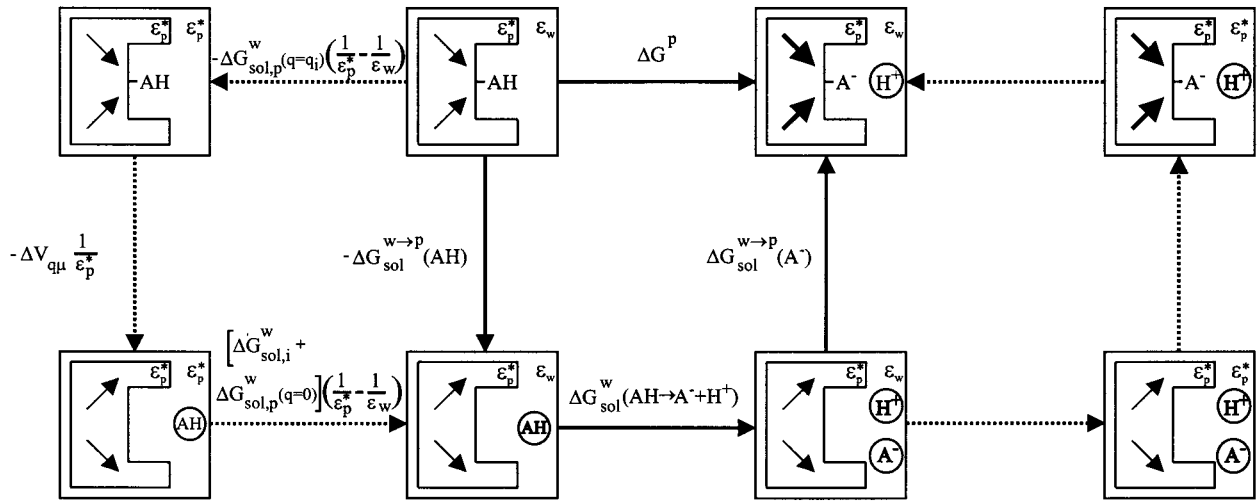


**Figure 3.** Thermodynamic cycle used to calculate the p$K_a$'s of ionizable residues. The central cycle (solid arrows) corresponds to a microscopic evaluation of the free energy change ($\Delta G$) associated with the ionization of an acid AH in a protein-water system. The $\Delta G^{w}_{sol}$ is the change in free energy of solvation in water for the given process, and $\Delta G^{w\rightarrow p}_{sol}$ is the difference between the free energy of solvation in water and protein for the indicated group. The coupled cycles (broken arrows) correspond to the semi-microscopic PDLD/S approach where $\Delta G^{w\rightarrow p}_{sol}$ is evaluated by changing the dielectric of the solvent from $\epsilon_w$ to $\epsilon^*_p$ (the $\epsilon^*_p$ is a scale factor that accounts for the interactions that are not considered explicitly). The $\Delta G^{w}_{sol,p}$ ($q = q_i$) and $\Delta G^{w}_{sol,p}$ ($q = 0$) terms are the free energies of solvation of the protein in water with atomic charges present on the particular group and with atomic charges on the group set to zero, respectively. $\Delta V_{q\mu}$ is the vacuum interaction between the atomic charges on the group and the permanent dipoles of the protein. The orientation and magnitude of these dipoles are affected by the presence and charge state of the ionizable group and indicated schematically by arrows.

a linear response approximation (LRA) calculation.[40,41] In the PDLD/S method the average polarization of the solvent is approximated by Langevin-type dipoles, and the interaction energies are scaled in a consistent way that increases the precision of the result. The free energy associated with moving the given group from water to the protein, which is fixed in a single configuration, can be calculated by using a coupled thermodynamic cycle (Figure 3, left and right cycles):

$$(\Delta G^{w\rightarrow p}_{sol,i})_s = [-\Delta G^{w}_{sol,i} + \Delta G^{w}_{sol,p}(q = q_i) - \Delta G^{w}_{sol,p}(q = 0)]\left(\frac{1}{\epsilon^*_p} - \frac{1}{\epsilon_w}\right) + \Delta V_{q\mu}\frac{1}{\epsilon^*_p} \quad (3)$$

where s indicates that a single protein configuration is used, $\Delta G^{w}_{sol,i}$ is the free energy of solvation of the ionizable group (the self-energy in water), $\Delta G^{w}_{sol,p}$ ($q = q_i$) and $\Delta G^{w}_{sol,p}$ ($q = 0$) are the free energies of solvation of the entire protein in water with atomic charges present on the particular group ("charged state") and with atomic charges on the group set to zero ("uncharged state"), respectively. The $\Delta G^{w}_{sol,p}$ ($q = 0$) term approximates the case where the ionizable group is not in the protein cavity. $\Delta V_{q\mu}$ is the vacuum interaction between the atomic charges on the ionizable group and the permanent dipoles of the protein (represented by atomic charges), $\epsilon_w$ is the dielectric constant of water, and $\epsilon^*_p$ is a scaling factor which accounts for the interactions that are not considered explicitly. This factor is quite different than the actual protein dielectric constant (see below and in ref 41).

To capture the physics of the reorganization of the protein dipoles in the charging process, it is necessary to relax the protein structure in the relevant charged and uncharged states. Moreover, for accurate free-energy differences, several protein configurations should be averaged. The phase space can be adequately sampled by utilizing Monte Carlo or molecular dynamics (MD) techniques.[42] In this study we use a MD approach in the LRA framework.[40,41] This approach approximates the free energy associated with a transformation between two charge states by averaging the potential difference between the initial and final states over trajectories propagated on these two states, respectively. Using the PDLD/S free energy that corresponds to a single protein structure as an effective potential in the PDLD/S-LRA method, the free energy of solvation is given by

$$\Delta G^{w\rightarrow p}_{sol,i} = \frac{1}{2}[\langle \Delta V^{w\rightarrow p}_{sol,i}\rangle_{q=q_i} + \langle \Delta V^{w\rightarrow p}_{sol,i}\rangle_{q=0}] \quad (4)$$

where the $\Delta V^{w\rightarrow p}_{sol,i}$ is the PDLD/S effective potential (the $(\Delta G^{w\rightarrow p}_{sol,i})_s$ of eq 3), the $\langle\ \rangle_{q=q_i}$ and $\langle\ \rangle_{q=0}$ terms designate an average over protein configurations generated in the charged and uncharged state of the given group, respectively. Although this approach takes into account the reorganization of the environment explicitly, it may not fully account for some effects such as the complete water penetration and protein reorganization. These factors and the effect of induced dipoles are implicitly included in the model, which lead to the use of $\epsilon^*_p = 4$ in this work.

Different strategies can be followed in calculating the p$K_a$ of a particular group in the protein, where several other ionizable groups are present. One solution is to fix the protonation states of the residues which are predominantly charged at physiological pH and calculate the charge−charge interactions in $\Delta G^{w\rightarrow p}_{sol,i}$ explicitly using the PDLD/S-LRA method. This approach takes into account the reorganization of charges in the ionization process and is useful when the ionizable groups are in close proximity to the group whose p$K_a$ is evaluated. Alternatively, one can consider the free energy change in two steps. In the first step, the ionizable group of interest is transferred from water to a protein environment where all other ionizable groups are in their neutral form (no assumption about the protonation states of other ionizable residues is needed). In this step all interactions of the atomic charges on the group with the dipoles of the protein and water are explicitly considered using the PDLD/S-LRA method. In the second step, the charge states of the ionizable residues are determined iteratively in a self-consistent manner. The charge−charge interactions are calculated using a macroscopic model where the reorganization of the protein and solvent is considered implicitly by using $\epsilon_{eff} = 40$ (the justification and validation of this approach is given elsewhere[43]). Here, the p$K_a$ in the protein is given by

(41) Sham, Y. Y.; Chu, Z. T.; Warshel, A. *J. Phys. Chem. B* **1997**, *101*, 4458−4472.

(42) Allen, M. P.; Tildesley, D. J. *Computer Simulation of Liquids*; Oxford University Press: Oxford, 1989.

(43) Sham, Y. Y.; Muegge, I.; Warshel, A. *Biophys. J.* **1998**, *74*, 1744−1753.

$$pK^{p}_{a,i} = pK_{int,i} + \sum_{i \neq j}(\Delta pK_{a,i})_j = pK^{w}_{a,i} + \frac{1}{2.3RT}(\Delta\Delta G^{w\rightarrow p}_{sol,i}) + \sum_{i \neq j}\Delta G^{p}_{ij} \quad (5)$$

where $pK_{int_i}$ is the intrinsic p$K_a$ of the ionizable group in the "neutral" protein, and $(\Delta pK_{a_i})_j$ is the p$K_a$ shift due to the charge on the $j$th ionizable residue. The intrinsic p$K_a$ can be expressed as in eq 2 by the p$K_a$ in water, $pK^{w}_{a,i}$, and $\Delta\Delta G^{w\rightarrow p}_{sol,i}$, which reflects the free-energy difference associated with moving the group in its ionized and neutral state from water to the "neutral" protein. The $\Delta G^{p}_{ij}$ represents all the charge−charge interactions in the protein. The accurate evaluation of the energetics of the intrinsic p$K_a$ in the first step is more important, since generally the protein−solvent environment effectively screens the charge−charge interactions.[44,45]

As a first step in the p$K_a$ calculations, we examined the accuracy of the solvation free energies ($\Delta G^{w}_{sol,i}$) of groups of interest. It should be noted, however, that only relative solvation energies are considered in our approach to obtain p$K_a$'s. The charges of the relevant groups were derived from ab initio HF/6-31G(d) calculations performed with the Gaussian 98 program.[46] This was done by fitting the charges to reproduce the molecular electrostatic potential and the total dipole moment of the molecule.[47] The calculated solvation free energies were found to be within 10% of the experimental data, and hence these charges were used in subsequent calculations throughout this work.

The molecular dynamics simulations of ALR2 that generated the protein structures for the LRA calculations started from the crystal structure of the cofactor-bound state of the enzyme (PDB entry 1ads).[16] The system was divided into two regions; the first (I) includes the side chain of the ionizable residue of interest (e.g., Tyr-48 or His-110), and the second (II) includes the surrounding protein and solvent environment. All region II atoms within 20 Å around the center of region I were subject to a weak constraint of 0.03 kcal mol$^{-1}$ Å$^{-2}$ around their crystal positions; atoms between 20 and 23 Å were constrained by 30 kcal mol$^{-1}$ Å$^{-2}$. All nonbonded interactions with atoms beyond 23 Å were excluded from the calculation. The system within 20 Å around the center was solvated by all-atom water molecules, which were subject to the boundary condition of the surface constraint all-atom solvent (SCAAS) model.[48] The solvent between 20 and 23 Å was represented by a grid of Langevin-type dipoles, and beyond 23 Å by a continuum with the dielectric constant of bulk water ($\epsilon = 80$). The long-range effects in this spherical SCAAS system were treated by the local reaction field (LRF) method.[49] The system set up this way allows for a reliable and consistent treatment of the electrostatic effects in the enzyme−solvent system.

The standard all-atom ENZYMIX parameters[40] were employed for the whole system, except for the region I charges (described above) and those on the NADPH cofactor in region II which were obtained from the CHARMM22 force field.[50,51] In the MD simulations the induced energies and forces were evaluated with charges scaled by a factor of 0.75 on non-ionized residues in region II. The PDLD/S-LRA simulations were carried out with the POLARIS/ENZYMIX program package.[40] The entire system was equilibrated at 300 K by a 5000 step molecular dynamics simulation with a 1 fs time step. In the subsequent 15 000 steps, 30 configurations were extracted for PDLD/S calculation every 500 steps.[40] The p$K_a$ value of a particular ionizable group was determined as the average of the p$K_a$ values calculated for the 30 single protein configurations. As the $\Delta G^{w\rightarrow p}_{sol}$ for AH was found to be small (<1 kcal/mol), this energy term was neglected in the present study. The effect of ionized residues in the protein environment on the p$K_a$ was evaluated both by using the charged residues in the protein explicitly and by using a macroscopic model.

**2.2. EVB-FEP Simulations.** Simulation techniques which determine the free energy along a reaction coordinate can provide valuable insight into the molecular details of enzymatic reactions.[38] Since chemical processes involve bond rearrangements, the quantum mechanical nature of the process must be included in the model. The empirical valence bond (EVB) method coupled with free energy perturbation (FEP) and umbrella sampling techniques offers an effective way to obtain quantitative results.[38] The capability of this method to provide reliable potential surfaces for hydride-transfer reactions in solution has been demonstrated earlier.[52] The EVB approach has been extensively discussed elsewhere,[38,53] and it is now used by several leading research groups.[54−67] Thus, we will only consider some general points of the methodology here.

In the EVB approach the system is divided into a reaction region (the EVB atoms) where electronic changes take place, and an environment region which perturbs the reaction region through electrostatic, van der Waals, and bonding interactions. The EVB Hamiltonian matrix includes diagonal elements ($H_{ii}$) which represent pure VB states and off-diagonal elements ($H_{ij}$) which represent the quantum mechanical coupling of these states. The ground-state energy of the system is calculated by diagonalizing the EVB Hamiltonian. The diagonal element (or the energy) of the $i$th VB state is described by force field-type potential functions and a constant, designated as $\alpha_i$. The force field-type functions are usually fitted to reproduce various experimental data. The constant $\alpha_i$ is the gas-phase energy of the $i$th state when all the EVB fragments are at infinite separation. The difference between $\alpha_i$ and $\alpha_j$ ("gas-phase shift") determines the relative energy of the VB states for a particular reaction step. To obtain reliable values for the gas-phase shifts, we adjust $\Delta\alpha_{ij}$ until the calculated EVB free energy change of a reference reaction reproduces the corresponding experimental value or ab initio quantum mechanical estimates. The $H_{ii}$'s of the EVB Hamiltonian obtained this way guarantee a reliable description of the reaction potential surface at its asymptotic regions.

(44) Rees, D. C. *J. Mol. Biol.* **1980**, *141*, 323−326.
(45) Warshel, A.; Russel, S. T. *Q. Rev. Biophys.* **1984**, *17*, 283−422.
(46) Frisch, M. J.; Trucks, G. W.; Schlegel, H. B.; Scuseria, G. E.; Robb, M. A.; Cheeseman, J. R.; Zakrzewski, V. G.; Montgomery, J., J. A.; Stratmann, R. E.; Burant, J. C.; Dapprich, S.; Millam, J. M.; Daniels, A. D.; Kudin, K. N.; Strain, M. C.; Farkas, O.; Tomasi, J.; Barone, V.; Cossi, M.; Cammi, R.; Mennucci, B.; Pomelli, C.; Adamo, C.; Clifford, S.; Ochterski, J.; Petersson, G. A.; Ayala, P. Y.; Cui, Q.; Morokuma, K.; Malick, D. K.; Rabuck, A. D.; Raghavachari, K.; Foresman, J. B.; Cioslowski, J.; Ortiz, J. V.; Stefanov, B. B.; Liu, G.; Liashenko, A.; Piskorz, P.; Komaromi, I.; Gomperts, R.; Martin, R. L.; Fox, D. J.; Keith, T.; Al-Laham, M. A.; Peng, C. Y.; Nanayakkara, A.; Gonzalez, C.; Challacombe, M.; Gill, P. M. W.; Johnson, B.; Chen, W.; Wong, M. W.; Andres, J. L.; Gonzalez, C.; Head-Gordon, M.; Replogle, E. S.; Pople, J. A. *Gaussian 98*, revision A.4; Gaussian, Inc.: Pittsburgh, PA, 1998.
(47) Singh, U. C.; Kollman, P. A. *J. Comput. Chem.* **1984**, *5*, 129−145.
(48) King, G.; Warshel, A. *J. Chem. Phys.* **1989**, *91*, 3647−3661.
(49) Lee, F. S.; Warshel, A. *J. Chem. Phys.* **1992**, *97*, 3100−3107.
(50) Pavelites, J. J.; Bash, P. A.; Gao, J.; MacKerell, A. D., Jr. *J. Comput. Chem.* **1997**, *18*, 221−239.
(51) MacKerell, J., A. D.; Bashford, D.; Bellott, M.; Dunbrack, R. L., Jr.; Evanseck, J. D.; Field, M. J.; Fischer, S.; Gao, J.; Guo, H.; Ha, S.; Joseph-McCarthy, D.; Kuchnir, L.; Kuczera, K.; Lau, F. T. K.; Mattos, C.; Michnick, S.; Ngo, T.; Nguyen, D. T.; Prodhom, B.; Reiher, I., W. E.; Roux, B.; Schlenkrich, M.; Smith, J. C.; Stote, R.; Straub, J.; Watanabe, M.; Wiorkiewicz-Kuczera, J.; Yin, D.; Karplus, M. *J. Phys. Chem. B* **1998**, *102*, 3586−3616.
(52) Kong, Y. S.; Warshel, A. *J. Am. Chem. Soc.* **1995**, *117*, 6234−6242.
(53) Åqvist, J.; Warshel, A. *Chem. Rev.* **1993**, *93*, 2523−2544.
(54) Kim, H. J.; Hynes, J. T. *J. Chem. Phys.* **1990**, *93*, 5194−5210.
(55) Kim, H. J.; Hynes, J. T. *J. Am. Chem. Soc.* **1992**, *114*, 10508−10528.
(56) Chang, Y.-T.; Miller, W. H. *J. Phys. Chem.* **1990**, *94*, 5884−5888.
(57) Chang, Y.-T.; Minichino, C.; Miller, W. H. *J. Chem. Phys.* **1992**, *96*, 4341−4355.
(58) Grochowski, P.; Lesyng, B.; Bala, P.; McCammon, J. A. *Int. J. Quantum Chem.* **1996**, *60*, 1143−1164.
(59) Bala, P.; Grochowski, P.; Lesyng, B.; McCammon, J. A. *J. Phys. Chem.* **1996**, *100*, 2535−2545.
(60) Neria, E.; Karplus, M. *Chem. Phys. Lett.* **1997**, *267*, 23−30.
(61) Hinsen, K.; Roux, B. *J. Comput. Chem.* **1997**, *18*, 368−380.
(62) Vuilleumier, R.; Borgis, D. *J. Phys. Chem. B* **1998**, *102*, 4261−4264.
(63) Schmitt, U. W.; Voth, G. A. *J. Phys. Chem. B* **1998**, *102*, 5547−5551.
(64) Sagnella, D. E.; Tuckerman, M. E. *J. Chem. Phys.* **1998**, *108*, 2073−2083.
(65) Okuyama-Yoshida, N.; Nagaoka, M.; Yamabe, T. *J. Phys. Chem. A* **1998**, *102*, 285−292.
(66) Åquist, J.; Fothergill, M. *J. Biol. Chem.* **1996**, *271*, 10010−10016.
(67) Kim, Y.; Corchado, J. C.; Villà, J.; Xing, J.; Truhlar, D. G. *J. Chem. Phys.* **2000**, *112*, 2718−2735.

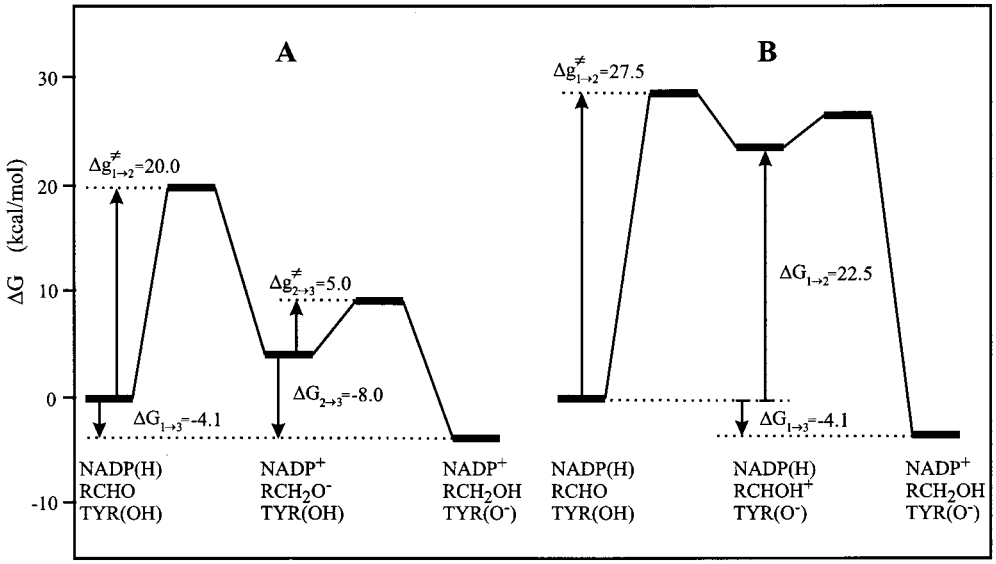


**Figure 4.** Free energy diagram for the reference reaction in water at pH = 7 with Tyr as a proton donor. The $\Delta G$s are the free energy changes, and the $\Delta g^{\ddagger}$s are the activation free energies for the transitions between the indicated states. Both the $\Delta G$s and the $\Delta g^{\ddagger}$s are deduced from experimental data. (A) The energetics of the mechanism that starts with a hydride transfer from NADPH to the substrate followed by a protonation of the intermediate anion; (B) The energetics of the mechanism that starts with a proton transfer from Tyr to the substrate followed by a hydride transfer from NADPH to the intermediate cation.

The $H_{ij}$'s can be adjusted similarly by fitting the calculated EVB barrier of a reference reaction to the corresponding experimental or theoretical estimate and by fitting the complete transition state region of the EVB surface to the corresponding ab initio surface. These parameters are then kept constant while moving the EVB atoms from the reference state to the protein environment. The reference reaction is generally the catalytic reaction performed in a water cage that includes the substrate and the catalytic groups. The mechanism of the catalytic reaction corresponds to the assumed mechanism in the enzyme and not necessarily to that in the solution. The use of such a reference reaction guarantees reliable energetics in enzyme modeling and allows one to determine the difference between the effects of the solvent and the protein environment. The corresponding difference in activation free energies gives the catalytic effect of the enzyme.[37] It is useful to point out that this approach uses a potential surface which is calibrated to reproduce the relevant free-energy surface of the reference solution reaction. The calibration also absorbs the nuclear quantum mechanical corrections of the reference reaction in the $H_{ij}$ term, but the possible difference between the nuclear quantum mechanical effects in solution and enzyme reactions is neglected. This difference is, however, usually minor.[37,68]

The free-energy profile of the reaction is evaluated by using a FEP/umbrella sampling technique. This approach uses a mapping potential ($V_m$) which is given in the simple two-state case by

$$V_m = H_{11}(1 - \lambda_m) + H_{22}\lambda_m \quad (6)$$

where $\lambda_m$ is a mapping parameter that drives the system from the reactant to the product state. The umbrella sampling procedure is then used to obtain the actual ground-state free energy (for details see ref 38). This reaction free energy is calculated along a reaction coordinate, which is taken as the energy gap between the two diabatic states, $H_{11}$ and $H_{22}$.

In the present study, the VB states used represented the reactant, possible intermediate, and product states. In each reaction step, the initial VB state was transformed into the final one in 21 FEP mapping steps. At each mapping step, the configuration space was explored with 3 ps simulation time at 300 K using 1 fs time steps. The stability of the simulations was tested by different initial conditions and longer simulation times, and the convergence error was assessed by forward and backward integration of the same trajectory. The effect on the final results, however, was small (<2 kcal/mol) since similar changes occur in the protein and in solution. The EVB-FEP simulations were first performed in water to calibrate the gas-phase shifts ($\Delta\alpha_{ij}$) and the off-diagonal matrix elements ($H_{ij}$) for the corresponding VB states against the relevant experimental data (see below). The same parameters were used in the simulation of the reaction in the protein environment. The treatment of the solvent, atomic charges, and the polarizable force field parameters were those described in section 2.1. The simulation of the catalytic reaction was performed using the ENZYMIX program.[40]

## 3.Results and Discussion

**3.1. Analysis of the Energetics of the Reference Solution Reaction.** Understanding catalytic reactions in enzyme active sites is one of the major challenges of biochemistry. Enzymes can accelerate chemical reactions compared to the same reaction in water due to their unique three-dimensional structure. Therefore, solution-phase reactions serve as suitable reference systems in theoretical studies of enzymes. In this section we attempt to give a careful analysis of the energetics of the reference solution reaction. The analysis will serve as a basis for the study of the catalytic reaction of ALR2. The results of this analysis are depicted in Figures 4 and 5 to help the reader follow the steps considered below.

We start our experimentally based analysis by considering the energetics of the overall reference reaction. This reaction can be written as

$$RCHO + NADPH + AH = RCH_2OH + NADP^+ + A^- \quad (I)$$

where RCHO and $RCH_2OH$ are the aldehyde reactant and alcohol product, respectively, and AH is the participating acid. A reliable estimate of the free energy of this reaction ($\Delta G_{1\to3}$) can be obtained by combining the relevant free energy changes using biochemical standard electrode potentials[69,70] at pH = 7. That is, for (R = Me) we have:

(68) Hwang, J.-K.; Warshel, A. *J. Am. Chem. Soc.* **1996**, *118*, 11745−11751.

(69) Sober, H. A. *Handbook of Biochemistry*; Sober, H. A., Ed.; CRC Press: Cleveland, OH, 1970.

(70) Fasman, G. D. *Practical Handbook of Biochemistry and Molecular Biology*; Fasman, G. D., Ed.; CRC Press: Boca Raton, FL, 1989.

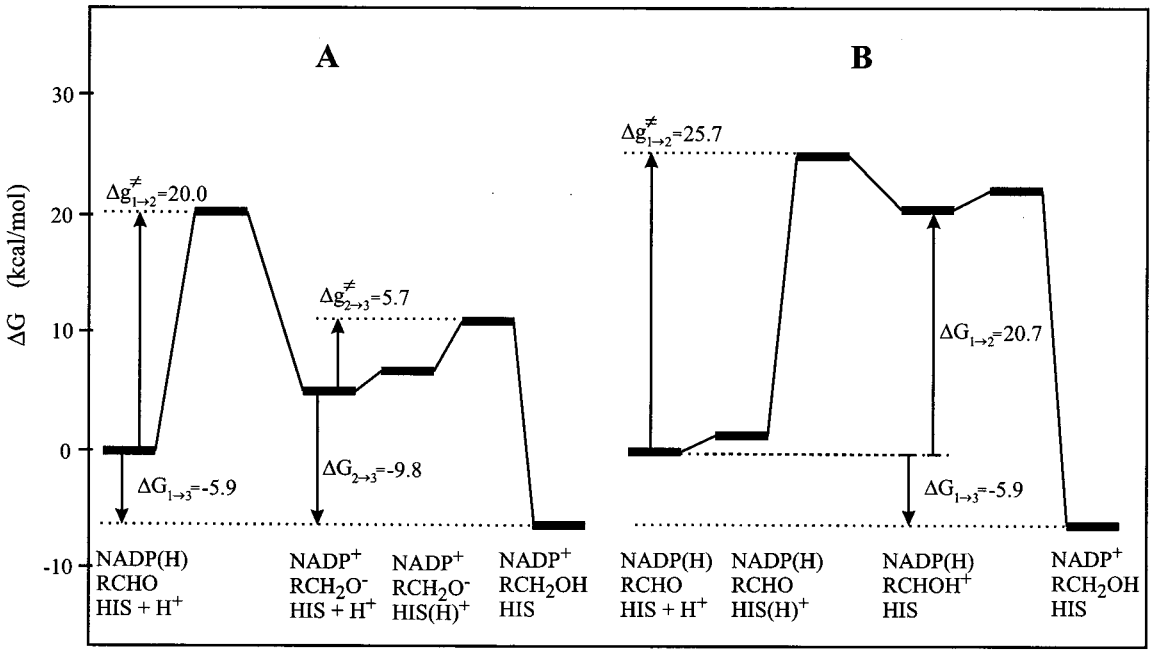


**Figure 5.** Free energy diagram for the reference reaction in water at pH = 7 with His as a proton donor. The $\Delta G$s are the free energy changes, and the $\Delta g^{\ddagger}$s are the activation free energies for the transitions between the indicated states. Both the $\Delta G$s and the $\Delta g^{\ddagger}$s are deduced from experimental data. Note that the protonation energy of His is included in the reaction energetics. (A) The energetics of the mechanism that starts with a hydride transfer from NADPH to the substrate followed by a protonation of the intermediate anion (B) The energetics of the mechanism that starts with a proton transfer from His to the substrate followed by a hydride transfer from NADPH to the intermediate cation.

$$RCHO + 2H^+ + 2e^- \rightarrow RCH_2OH \qquad \Delta G^{\circ\prime}_{red} = 2\Phi \times 0.197\ V \quad (II)$$

$$NADPH \rightarrow NADP^+ + H^+ + 2e^- \qquad \Delta G^{\circ\prime}_{ox} = -2\Phi \times 0.324\ V \quad (III)$$

combining these equations we obtain

$$RCHO + NADPH + H^+ = RCH_2OH + NADP^+ \qquad \Delta G^{\circ\prime}_{emf} = -2\Phi \times 0.127\ V \quad (IV)$$

where $\Phi = 23.06$ kcal mol$^{-1}$ V$^{-1}$

The electromotive force (emf) of the above cell, $\Delta G^{\circ\prime}_{emf}$ gives $-5.9$ kcal/mol at the biochemical standard state (pH = 7); that is, $\Delta G^{\circ}_{emf} = \Delta G^{\circ\prime}_{emf} - 2.3RT(7 - pH) = -15.6$ kcal/mol at the chemical standard state (pH = 0). To take into account the nature of the proton donor, one has to consider the deprotonation (DP) energy of the proton source in the system. The relevant reaction and the corresponding free energy can be written as $AH \rightarrow A^- + H^+$ and $\Delta G^{\circ}_{DP} = 2.3RT(pK_a - pH)$, respectively. We also need to consider the energetics of bringing the molecules into the same solvent cage and the change in electrostatic interactions between the reacting molecules during the chemical process. This free-energy correction ($\Delta G_C$) for the electrostatic attraction was estimated earlier[45] using a dielectric constant of 30. The corresponding results are $\sim -2.5$ kcal/mol for bringing two oppositely charged groups to around 3 Å and $\sim 0$ kcal/mol for interactions between charged and neutral species. Finally, the overall energy of eq I ($\Delta G_{1\rightarrow3}$) is obtained by combining the relevant energy terms. The resulting free-energy change is $\Delta G_{1\rightarrow3} = \Delta G^{\circ}_{emf} + 2.3RT(pK_a) + \Delta G_C$. This equation is pH-independent, but it depends on the $pK_a$ of the proton donor.[70] Thus, we obtain $\Delta G_{1\rightarrow3} = -15.6 + 1.38 \times 10.1 - 2.5 = -4.1$ kcal/mol for tyrosine (Figure 4) and $\Delta G_{1\rightarrow3} = -15.6 + 1.38 \times 6.5 = -6.6$ kcal/mol for histidine. However, for a doubly protonated histidine we should consider a small energy of the initial protonation at pH = 7 ($pK_a \approx 6.5$), $\Delta G^{\circ}_{p} = -2.3RT(pK_a - pH)$. Thus, the free energy of the overall process in water with histidine as the reactive acid is $\Delta G_{1\rightarrow3} = -6.6 + 1.38 \times 0.5 = -5.9$ kcal/mol at pH = 7 (Figure 5).

The free energy of the proton transfer (PT) step can also be estimated[45] by using experimental $pK_a$ values[70] for the donor and acceptor groups in solution. Using $\Delta G_{PT}$ and $\Delta G_{1\rightarrow3}$ we obtain the free energy of the intermediate structures (for histidine the initial protonation free energy, $\Delta G_P = 0.7$ kcal/mol at pH = 7, should also be considered). In a mechanism, where the protonation of the anionic intermediate terminates the catalytic reaction, we obtain the free energy of the proton-transfer step by $\Delta G_{PT} = 2.3RT[pK_a(AH) - pK_a(RCH_2OH)] + \Delta G_C$. This gives for tyrosine $1.38(10.1-15.9) = -8.0$ kcal/mol (Figure 4a) and for histidine $1.38(6.5-15.9) + 2.5 = -10.5$ kcal/mol (Figure 5a). In this mechanism the hydride transfer gives an ion pair intermediate with $\Delta G_{1\rightarrow2} = 3.9$ kcal/mol. This result does not depend on the nature of the proton donor in the vicinity of the intermediate due to the electrostatic screening of water. In an alternative mechanism the protonation of the substrate carbonyl oxygen initializes the catalytic step with $\Delta G_{PT} = 2.3RT[pK_a(AH) - pK_a(RCHOH^+)] + \Delta G_C$. In the absence of an experimentally available $pK_a$ for aliphatic aldehydes, we use in this work an estimate of $pK_a = -8$ based on the $pK_a$'s of aliphatic ketones.[71] The corresponding proton-transfer processes require $1.38(10.1 + 8.0) - 2.5 = 22.5$ kcal/mol and $1.38(6.5 + 8.0) = 20.0$ kcal/mol for tyrosine and histidine, respectively. This gives for the corresponding cationic intermediates $\Delta G_{1\rightarrow2} = 22.5$ kcal/mol (Figure 4b) and $\Delta G_{1\rightarrow2} = 20.7$ kcal/mol (Figure 5b), respectively. Hence, the system has to overcome a large free energy increase due to the weak basicity of aliphatic aldehydes.

The activation free energies of the relevant reaction steps in solution can be estimated from free-energy relationships based

(71) Arnett, E. M. *Prog. Phys. Org. Chem.* **1963**, *1*, 223−393.

on experimental data.[38] Proton transfer barriers are approximately 5 kcal/mol higher than the free-energy change of the actual process in water. The activation free energy for a hydride transfer to the carbonyl substrate is approximately 20 kcal/mol.[52,72] The barrier to transfer the hydrogen from NADPH to the protonated substrate is expected to be lower than the preceding proton-transfer barrier.

In summary, the analysis of the energetics of the reference reaction shows (Figures 4 and 5) that the mechanism with an initial proton transfer involves a large activation barrier and it is unlikely to proceed with a reasonable rate in solution. On the other hand, the mechanism with an initial hydride transfer to the substrate involves a relatively low activation barrier. More specifically, the barrier to the initial hydride transfer is ~20 kcal/mol, and the barrier to the subsequent protonation is ~5 kcal/mol. In the case that histidine is the proton donor, an initial protonation free energy of ~0.7 kcal/mol at pH = 7 should also be considered. Finally, it is worth noting that the calculated catalytic efficiency of an enzyme does not depend greatly on the accurate energetics of the reference reaction in water but rather on the difference between the energetics of the solution and enzyme reactions. Nevertheless, we feel that our estimate of the free-energy changes in water is sufficiently reliable to allow one to obtain a quantitative description of the absolute free-energy changes in the enzyme.

**3.2. Analysis of the Energetics of the Catalytic Step in the Enzyme.**

**3.2.1. Calculations of p$K_a$'s in the Wild-Type Enzyme.** To evaluate the energetics of the reaction in the enzyme, we need to determine the free energy required to transfer the system from water to the protein interior. This can be done by calculating the solvation free energies of the participating fragments in water and in the protein. The relevant $\Delta G_{sol}^{w\rightarrow p}$ values enable us to evaluate the p$K_a$'s of important groups in the active site of the enzyme. For example, it was suggested[30] that in ALR2 His-110 is the acid−base catalyst with a p$K_a$ ~7 based on pH dependent steady-state kinetic parameters. However, others[16] argued that the p$K_a$ of His-110 is abnormally low based on structural considerations. In this case His-110 would not be protonated in the enzyme and thus could not act as a proton donor. Several differing p$K_a$ shifts have been suggested[16,30] for the p$K_a$ of Tyr-48 as well, but a pH-dependent kinetic measurement[31] indicated that Tyr-48 has a p$K_a$ of 8.25. Our theoretical estimate of p$K_a$ values is based on a well-defined physical model, and thus it offers a reliable way to resolve these controversies. The calculated $\Delta G_{sol}^{w\rightarrow p}$ values and the corresponding p$K_a$'s are summarized in Table 1.

The p$K_a$'s of Tyr-48 and His-110 were evaluated by the two approaches described in section 2.1. The first one calculates the intrinsic p$K_a$ of the ionizable group and then determines the effect of other ionized residues by a consistent macroscopic approach. The other approach considers the ionized residues of the protein explicitly in the LRA procedure. The ionization states in this model were assigned on the basis of solution-phase p$K_a$ values that may not reflect the exact protonation states in the protein. However, the two approaches give similar results, and this indicates that the charge−charge interactions in the protein are relatively small. The $\Delta G_{sol}^{w\rightarrow p}$ for Tyr-48 is negative, which shows that the protein environment stabilizes the tyrosinate anion more effectively than water does. The relative free energy of −2.2 kcal/mol corresponds to a p$K_a$ of 8.5 which is in line with the experimentally predicted low p$K_a$ of Tyr-48. Analysis of the individual group contribution to the overall effect indicates that Lys-77 provides a strong electrostatic stabilization to the tyrosinate (for proper evaluation of the electrostatic effect of Lys-77, see mutation studies below). The aspartate residue, which destabilizes the anion, probably has a role in the positioning of the highly flexible Lys-77 in the vicinity of Tyr-48.

**Table 1.** Calculated p$K_a$ Values for Wild Type (WT) and Mutant Enzymes[a]

| residue | $\Delta G_{sol}^{w\rightarrow p}$ | p$K_i$ | $\Sigma(\Delta pK_a)_j$ | p$K_a$ |
|---|---|---|---|---|
| WT-Tyr48[b] | −0.83 ± 0.97 | 9.5 ± 0.7 | −1.03 | 8.5 ± 0.7 |
| WT-Tyr48[c] | −2.21 ± 1.38 | 8.5 ± 1.0 | − | 8.5 ± 1.0 |
| WT-His110[b] | 8.90 ± 1.28 | 0.0 ± 0.9 | 0.87 | 0.9 ± 0.9 |
| WT-His110[c] | 8.67 ± 1.24 | 0.2 ± 0.9 | − | 0.2 ± 0.9 |
| WT-His110[c,d] | 7.49 ± 2.32 | 1.1 ± 1.7 | − | 1.1 ± 1.7 |
| K77M-Tyr48[c] | 3.58 ± 1.38 | 12.7 ± 1.0 | − | 12.7 ± 1.0 |
| Y48H-Wat[c] | −3.70 ± 2.10 | 13.0 ± 1.5 | − | 13.0 ± 1.5 |
| barnase-His18[c,e] | −2.10 ± 0.54 | 8.0 ± 0.4 | − | 8.0 ± 0.4 |

[a] Notations as in eqs 3 and 5; the $\Delta G_{sol}^{w\rightarrow p}$ values in kcal/mol; the p$K_a$ values were determined as the average of 30 p$K_a$ values corresponding to protein configurations extracted from LRA MD simulations. The relevant solvation energies are averaged over the potential surfaces of the charged and uncharged states of the given residue; standard deviations are indicated. [b] The p$K_a$ was evaluated as the sum of the p$K_a$ in a "neutral" protein (p$K_i$) and the p$K_a$ shift ($\Sigma(\Delta pK_a)_j$) due to the effect of charges on other residues. The charge states were determined self-consistently and the charge−charge interactions are evaluated by a macroscopic approach with $\epsilon_{eff} = 40$. [c] The p$K_a$ was evaluated in a protein with pre-set ionization states. [d] The p$K_a$ was evaluated in a protein with crystallographic water molecules present. [e] The p$K_a$ of His-18 in barnase was evaluated to assess the accuracy of our method to calculate p$K_a$ of histidines in protein; the experimental p$K_a$ is 7.8.[74]

The $\Delta G_{sol}^{w\rightarrow p}$ value for the other potential proton donor, His-110, is around 8.7 kcal/mol (Table 1). This indicates that protonation of His-110 in the relatively hydrophobic environment is greatly unfavorable process compared to the corresponding process in water (the p$K_a$ is shifted down by 6 units; see our validation study in ref 73). The effect of the crystallographic water molecules on the p$K_a$ of His-110 was investigated explicitly (these molecules are represented in the other calculations by Langevin dipoles). It was found that the protonation of His-110 is also greatly unfavorable in this model. The possibility of a neutral histidine as a proton donor in the system was considered as well. A neutral histidine was proposed to act as a general acid in the catalytic reaction of triosephosphate isomerase.[75] However, the imidazolate anion in ALR2 is destabilized relative to water (the corresponding $\Delta G_{sol}^{w\rightarrow p}$ value is calculated to be 4.5 kcal/mol), and this further increases the p$K_a$ of a neutral histidine[70] from the aqueous p$K_a$ of 14.5. Thus, it appears that in the specific environment of this enzyme neither a neutral nor a protonated histidine can play the role of a proton donor.

The p$K_a$ of the potential proton donor groups in the presence of a substrate cannot be investigated without considering the given acceptor group in the process. The best way is to examine the actual proton transfer in the protein environment, where the

(72) Yadav, A.; Jackson, R. M.; Holbrook, J. J.; Warshel, A. *J. Am. Chem. Soc.* **1991**, *113*, 4800−4805.

(73) To verify the reliability of the calculated shift in the p$K_a$ of His-110 in ALR2, we investigated a system where the p$K_a$ of a histidine in a protein environment is experimentally established. We chose barnase (PDB entry 1bni), where the p$K_a$ of His-18 has been shown[74] to be unusually high (p$K_a$ = 7.8) due in part to the stabilizing interaction with Trp-94. Our PDLD/S-LRA calculations using the described simulation protocol showed that the protonated histidine is stabilized in the protein relative to water and gave a p$K_a$ of around 8 (see Table 1). The encouraging results indicate that the method applied here reflects the experimentally observed effects well.

(74) Lowenthal, R.; Sancho, J.; Fersht, A. R. *J. Mol. Biol.* **1992**, *224*, 759−770.

(75) Bash, P. A.; Field, M. J.; Davenport, R. C.; Petsko, G. A.; Ringe, D.; Karplus, M. *Biochemistry* **1991**, *30*, 5826−5832.

proton donor and acceptor groups are treated together by the PDLD/S-LRA method. The calculated $\Delta G_{sol}^{w\rightarrow p}$ values should indicate whether the proton transfer is energetically favored in the protein relative to water. The intermediate complexes $Tyr(O^-)\cdot RCHOH^+$ and $His\cdot RCHOH^+$ are destabilized in ALR2 relative to water by 6.3 and 10.8 kcal/mol, respectively. These $\Delta G_{sol}^{w\rightarrow p}$ values should, however, be compared to those of the initial state of the complexes, which are 1.6 and 11.1 kcal/mol for $Tyr(OH)\cdot RCHO$ and $HisH^+\cdot RCHO$, respectively. As a result, the energetics of the initial proton transfer from Tyr-48 to the substrate is less favorable by 4.7 kcal/mol in the protein than in solution. In the case that the histidine is the proton donor, the reaction energetics in the protein is slightly lower than that in solution (−0.3 kcal/mol). Thus, the high energy of the system due to the initial protonation of His is somewhat lowered by the relocation of the proton from His to the substrate. However, the initial proton-transfer step has been shown to require prohibitively high energy in water, and in light of the present results, this remains the case in the protein. The other mechanism, in which the hydride transfer initiates the catalytic step, involves the ion pair $NADP^+\cdot RCH_2O^-$ that is also destabilized in the active site compared to the same system in water.

An analysis of the structures obtained with the MD simulations of the binary and ternary complexes shows that the imidazole ring of His-110 rocks freely in the absence of a substrate in the active site, but upon substrate binding it participates in the stabilization of the substrate through hydrogen bonds. This observation is in line with the hypothesis that a neutral His-110 protonated on N$\epsilon$2 plays a role in the recognition of polar 2-D-hydroxyaldehyde substrates (e.g., D-glyceraldehyde, D-glucose) in the active site.[21] Without a substrate in the active site, the tyrosine hydroxyl is oriented toward Asp-43, away from the active site. This orientation changes upon substrate binding and catalysis, where this hydroxyl plays an active role.

The results given above show how different functionally important charges are solvated in the protein active site relative to water. It appears that ALR2 has not evolved to accommodate a positive charge in the active site. It better solvates ion pairs but not as well as water does. Finally, neutral species are solvated similarly in the protein and in water. We have indirect information about the solvation of a negative charge by ALR2; that is, there are crystal structures of complexes of ALR2 with anionic species which suggest a specific anion-binding position in the active site.[17,18,22] However, the active conformation of the enzyme (*E) contains the oxidized cofactor, $NADP^+$, at pH = 5 where the crystal was obtained. Kinetic studies[31] show that the binding of DL-mandalate anion to $*E\cdot NADP^+$ is clearly favored over binding to *E·NADPH. Furthermore, Tyr-48 should also be protonated providing an extra stabilization to an anion through a hydrogen bond. The configuration of the ternary complex with anionic species, $*E\text{-}Tyr48(OH)\cdot NADP^+\cdot$anion, is believed to resemble the transition state configuration of the catalytic reaction.[31] Indeed, in the intermediate state where the negatively charged substrate $RCH_2O^-$ is in the active site, the $*E\cdot NADP^+$ environment provides stabilization to this anionic species (the corresponding $\Delta G_{sol}^{w\rightarrow p}$ value is calculated to be −3.7 kcal/mol). However, in the catalytic process the neutral substrate binds to the *E·NADPH and a charge separation occurs during the hydride transfer from the cofactor to the substrate. In this case the energetics of both reacting fragments should be considered, as was done above for the $NADP^+\cdot RCH_2O^-$ ion pair.

In summary, considering the fact that the protonation free energy of histidine is 0.7 kcal/mol in water at pH = 7, the charging process of His-110 demands around 9.4 kcal/mol in the protein, which makes it a very unlikely proton source in the catalytic step. Moreover, after the protonation of histidine, the proton transfer to the neutral substrate would require an additional 20 kcal/mol of free energy. This proton transfer from Tyr-48, which is protonated at physiological pH, requires an even larger free energy change ($\Delta G_{1\rightarrow 2} = 27.2$ kcal/mol). Thus, despite the fact that in the consecutive step the barrier for hydride transfer is low, an initial proton transfer to the substrate should be precluded. The alternative mechanism with an initial hydride transfer to the substrate is more viable in the protein environment, although the intermediate complex is at a higher energy relative to the corresponding energy in water. The subsequent proton transfer is expected to proceed at a lower energy than hydride transfer, which essentially rules out His-110 as a proton donor in the system.

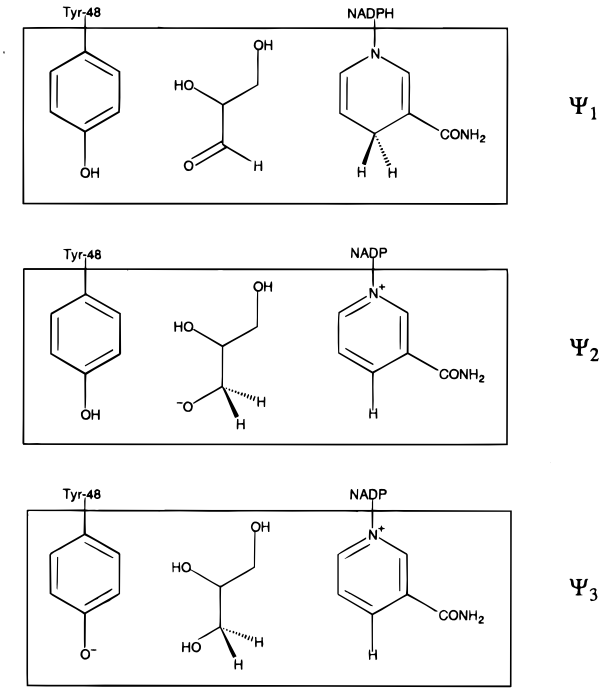


**Figure 6.** Valence bond structures used to describe the catalytic reaction of ALR2 corresponding to reactant ($\Psi_1$), intermediate ($\Psi_2$), and product ($\Psi_3$) states. The atoms shown in boxes are defined as EVB atoms.

**3.2.2. EVB-FEP simulations.** In the previous section we used $pK_a$ calculations to explore the nature of possible proton donors and the energetics of alternative pathways in the catalytic reaction of ALR2. It was found that Tyr-48 is the most probable proton source in the system. Furthermore, it was established that a mechanism where the hydride transfer precedes the proton-transfer step is favored. However, this does not give information about the activation free energies and the detailed reaction pathway in the enzyme. Thus, we examine here the free energy surface of the stepwise mechanism using EVB−FEP simulations, where a hydride transfer to D-glyceraldehyde takes place first, followed by a proton transfer from Tyr-48.

Three VB states were used to describe the two-step process, in which the EVB atoms included the phenol moiety of Tyr-48, the nicotinamide fragment of NADPH and the substrate, D-glyceraldehyde (Figure 6). The EVB calculations were calibrated using the relevant estimates for the $\Delta G$s and $\Delta g^{\ddagger}$'s of the reference reaction in solution (see section 3.1). The corresponding EVB parameters are $\Delta\alpha_{12} = 16$ kcal/mol, $H_{12} = 47$ kcal/mol and $\Delta\alpha_{23} = -21$ kcal/mol, $H_{23} = 12$ kcal/mol

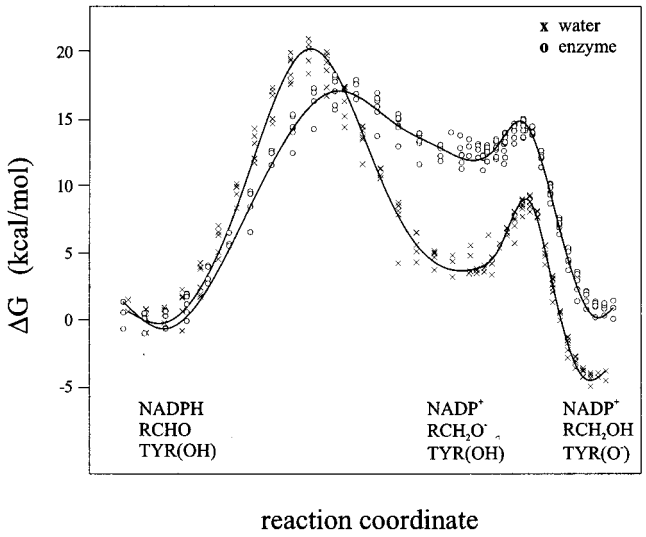


**Figure 7.** Free-energy profiles for the catalytic reaction in water (×) and protein (○) calculated with the EVB-FEP method. The reaction coordinate is taken as the energy gap between the two diabatic states, $H_{11}$ and $H_{22}$ (see text for details).

for the hydride- and proton-transfer steps, respectively. Here we use constant $H_{ij}$'s as the present results were found to be rather insensitive to the functional form of these off-diagonal elements (see ref 52 for a related analysis). The calculated free-energy profiles for the reaction in water and in the enzyme are summarized in Figure 7. In water, the hydride transfer to D-glyceraldehyde involves a 20 kcal/mol barrier and yields the intermediate ion pair $NADP^+ \cdot RCH_2O^-$ (R= $HO-CH_2-CH(OH)-$). A subsequent protonation through a 5 kcal/mol barrier terminates the reaction and gives the product configuration, Tyr48-$(O^-)\cdot NADP^+\cdot$alcohol. A comparison of the activation free energies of the hydride transfer in water and in the protein shows that the enzyme reduces the initial activation barrier by ~3 kcal/mol. At the same time, the intermediate state is less stable in the protein than in water by ~8 kcal/mol, in accord with the prediction of the PDLD/S-LRA method. The stabilization of the transition state and the destabilization of the intermediate state may seem contradictory. However, the energy of the transition state can be lowered not only through the stabilization of the intermediate state, but also through the smaller reorganization energy of the environment.[38] The relative free energies of the transition states along the free-energy pathway in water show that in this reference system the rate-limiting step is the hydride transfer. In ALR2, however, the transition states of both the hydride and proton transfers lie close enough to each other (~2 kcal/mol) that both can contribute to the apparent rate of the catalytic process. Indeed, large isotope effects were measured[21,76] for both hydride and proton transfers in the wild-type enzyme, and this supports our theoretical results.

A possible concerted mechanism was also simulated in order to determine whether the enzyme offers additional stabilization to the transition state in this reaction pathway. The simulation used two VB states corresponding to the reactant and product configurations. The EVB surface was calibrated using the experimental estimate for $\Delta G_{1\rightarrow3}$ in solution, which gave $\Delta\alpha_{12} = -5$ kcal/mol. Preliminary results indicate that the enzyme does not stabilize the transition state effectively. However, to obtain quantitative value for the free energy barrier in a concerted mechanism in the enzyme, the barrier in the corresponding reference reaction in solution must be determined. This information cannot be derived from experimental data, and it is the subject of a separate study using ab initio electronic structure calculations.

The energetics of the catalytic reaction can be better understood by constructing a free-energy diagram for the overall enzymatic process by using the estimated rate constants from experimental studies[76] (Figure 8). The rate-determining step of the overall process is the $*E-A^-\cdot NADP^+ \rightarrow E-A^-\cdot NADP^+$ isomerization with an experimental barrier of 18.5 kcal/mol. At the same time, kinetic isotope effect measurements indicate that the catalytic reaction contributes also to the apparent rate in the enzyme. This would suggest that the barrier to transform the aldehyde substrate to alcohol is around 15−17 kcal/mol. Our free-energy simulations give an activation barrier of ~17 kcal/mol in a reasonably good agreement with the experimental value of 14.8 kcal/mol calculated from kinetic constants. The calculated free-energy change of the catalytic reaction in the enzyme is ~0 kcal/mol which is close to the experimental value of −3 kcal/mol shown in Figure 8. It should, however, be noted that this experimental value is based on the rate of the reverse reaction in the enzyme that is considered[76] approximate at this time. Our calculations indicate that the enzyme does not significantly enhance the rate of the catalytic reaction with D-glyceraldehyde compared to the corresponding reaction in a water cage; that is, the transition state is stabilized by only 3 kcal/mol relative to water. This behavior is consistent with the proposed physiological role of ALR2 in detoxification,[10,11] namely, this enzyme can bind structurally diverse carbonyl containing substrates through the hydrogen bonds between the carbonyl oxygen and polar residues Tyr-48 and His-110, while the large active site accommodates the remainder of the substrates. This arrangement of an active site enables the proximity of the substrate, NADPH, and Tyr-48 to react in a stereospecific manner. As a result, ALR2 reduces a broad range of substrates at a moderate rate, in contrast with other enzymes, which produce a large rate enhancement in the conversion of a specific molecule. This point will be further discussed in the last section of the present work.

**3.2.3. Mutation Experiments.** Site-directed mutagenesis experiments have contributed significantly to the understanding of the mechanism of action in ALR2. For example, the reduced but measurable catalytic activity in His-110 mutants[21,27] essentially rules out the possibility that His-110 is a unique proton donor in the system. On the other hand, mutation of Tyr-48 to phenylalanine (Y48F)[21] resulted in a total loss of the enzymatic activity, which suggests that this residue is the proton donor in the catalytic reaction. Other mutants of Tyr-48, including serine (Y48S) and histidine (Y48H), retained some catalytic activity, which was explained[21] by the presence of a bound crystal water molecule in the active site, acting as the proton source. The crucial Lys-77•Tyr-48 interaction has also been examined by mutation of Lys-77 to methionine (K77M),[21] and as anticipated it yielded an inactive enzyme.

Although these experimental data give valuable information about the importance of specific residues in the catalytic process, the actual molecular basis for the change in the catalysis can be due to several factors other than the direct interaction between the given residues. Computer modeling of mutation studies can augment experimental information and help to establish the origin of the observed effects. However, simulations of mutation effects are very challenging, and a proper description should compare the free-energy path for the catalytic reaction in the wild-type and mutant enzymes.[77] Here, we only attempt to

(76) Grimshaw, C. E.; Bohren, K. M.; Lai, C., -J.; Gabbay, K. H. *Biochemistry* **1995**, *34*, 14356−14365.

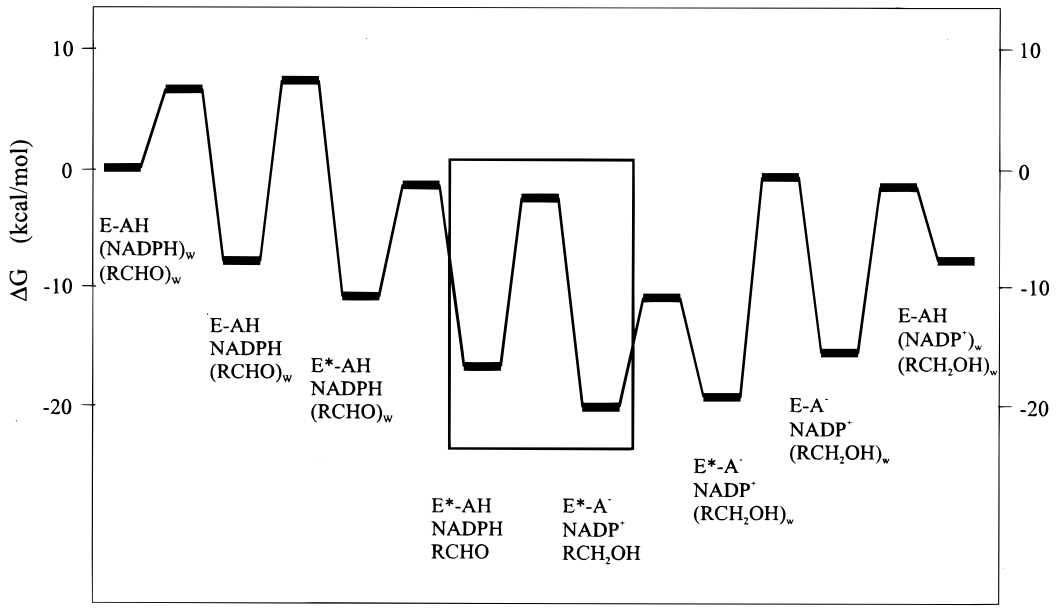


**Figure 8.** Free-energy diagram for the overall enzymatic process constructed by using kinetic data from experimental studies with D-xylose as a substrate (see text for details). The catalytic step studied in the present work is shown in a box.

estimate the effect of mutation on the energetics of the reaction by calculating p$K_a$ values for Tyr-48 in the K77M mutant and for the bound water molecule in the Y48H mutant.

The K77M mutant structure was built from the wild-type structure[16] by replacing Lys-77 with Met. This side-chain was subsequently relaxed in the protein environment. The p$K_a$ calculation was carried out using the same simulation protocol outlined in section 2.1. The results show that the tyrosinate anion is destabilized in the active site of the mutant by ∼3.6 kcal/mol relative to water (Table 1). The elevation of p$K_a$ from 8.5 to 12.7 represents ∼5.8 kcal/mol energy increase for a possible proton transfer as compared with the wild-type enzyme. The destabilization comes mainly from the electrostatic repulsion of the nearby Asp-43 which is not "neutralized" by Met-77 in the mutant as effectively as by Lys-77 in the wild-type enzyme. It has to be noted, however, that this effect cannot be attributed solely to the Lys-77 residue, because other consequences of the mutation, such as the observed increase in the distance between Asp-43 and Tyr-48, also contribute to the net effect. The reorganization of the surroundings can also be viewed as a part of the effective dielectric constant for the charge−charge interaction between Asp-43 and Tyr-48 (see ref 43). Nevertheless, the p$K_a$ shift clearly explains the experimental finding of an inactive K77M mutant and confirms the crucial role of Lys-77 in lowering the p$K_a$ of Tyr-48. A possible role of Asp-43 in the Tyr-48•Lys-77•Asp-43 triad can be the structural stabilization of the flexible Lys-77 in the vicinity of Tyr-48.

To consider the possible role of a reactive water molecule in the Y48H mutant, we evaluated the p$K_a$ of the crystal water in the enzyme. This calculation used the corresponding crystal structure (PDB entry 2acu).[21] The PDLD/S-LRA results indicate that the $OH^-$ anion formed upon the dissociation of the reactive water is stabilized in the mutant active site by ∼−3.7 kcal/mol relative to bulk water. This lowers the p$K_a$ of this water molecule from 15.7 to 13.0 (Table 1). Preliminary calculations of the p$K_a$ of His-48 in this mutant were carried out in order to determine whether the histidine can account for the residual activity observed in this mutant. However, a $\Delta G_{sol}^{w\rightarrow p}$ value of 7.2 kcal/mol shows that the doubly protonated form of His-48 is improbable in the protein. In light of these results, it seems that the experimentally observed water molecule may act as a proton donor in the system.

## 4. Concluding Remarks

This work explored the catalytic mechanism in human aldose reductase by computer simulation approaches. It has been established by the semi-microscopic PDLD/S-LRA method that the protonation of the potential proton donor His-110 prior to the catalytic process requires around 9 kcal/mol. Consequently, His-110 is not protonated in the active site of ALR2. Other theoretical studies,[29,32] which overlooked the energetics of the initial protonation, concluded that His-110 in its protonated form is the favored proton donor in the system. The reason for the low activation barriers obtained in the previous studies was the reduction of the unfavorable interactions of the charged His-110 with its protein environment during the forward reaction. However, it is clear from the present work that the energetics of the initial ionization state of His-110 must be considered in order to obtain a correct description of the catalytic mechanism. The p$K_a$ of the other potential proton donor, Tyr-48, was calculated to be around 8.5 in the active site of the enzyme. This is in accord with the proposed[16] stabilizing effect of the local environment of Tyr-48 and its experimentally determined p$K_a$ of 8.25.[31] Therefore, we conclude that Tyr-48 acts as the proton donor in the catalytic step of human aldose reductase.

Mutagenesis studies further highlight the importance of individual residues in the catalytic mechanism. The calculated p$K_a$ for Tyr-48 in the K77M mutant (∼12.7) established the essential role of Lys-77 in the stabilization of the tyrosinate anion in the relatively nonpolar active site and explains the experimentally observed lack of activity of this mutant. The water molecule identified in the active site of the Y48H mutant may account for its residual catalytic activity; that is, the p$K_a$ of this water is reduced by the mutant so that this molecule can serve as an alternative proton donor when Tyr-48 is mutated to another group. Although it is difficult to assess the effect of mutations on the proton-transfer barrier without detailed calculations, the available kinetic constants for the His-110 mutants[21]

(77) Warshel, A.; Sussman, F.; Hwang, J.-K. *J. Mol. Biol.* **1988**, *201*, 139−159.

show that $k_{cat}$ is reduced in these mutants by only a factor of 2−14, which is equivalent to a 0.4−1.6 kcal/mol increase in the overall activation barrier. The large protonation energy of His-110 in the wild-type enzyme and the 600−4200-fold increase in $K_m$ of His-110 mutants[21] imply that the neutral form of His-110 contributes to catalysis by increasing $k_{cat}/K_m$ via an enhancement of the binding of both the ground and transition states of the substrate.

Our detailed analysis of the reference reaction in solution showed that the stepwise mechanism where the protonation precedes hydride transfer is disfavored over the alternative stepwise mechanism. Furthermore, PDLD/S-LRA calculations indicated that an initial proton transfer step would require prohibitively high energy in the actual protein environment. Therefore, the most probable sequence of elementary steps in the catalytic reaction commences with the hydride shift to the substrate followed by the proton transfer from Tyr-48. The actual free-energy profile for the catalytic reaction has been obtained by the EVB−FEP method in a water cage and in the protein environment. The results show that in water the activation barrier to hydride shift is ∼20 kcal/mol, while the subsequent proton-transfer barrier lies ∼10 kcal/mol lower. The protein environment lowers the hydride-shift barrier by ∼3 kcal/mol relative to the corresponding barrier in a water cage and raises the proton-transfer barrier to within 2 kcal/mol of the hydride-shift barrier by destabilizing the intermediate state. Consequently, the barrier to convert the aldehyde substrate to alcohol is around 17 kcal/mol, and both reaction steps contribute to the apparent rate of the catalytic reaction. These results are in a quantitative agreement with the available experimental data.[21,76] Preliminary studies of a concerted mechanism suggest that the enzyme does not offer stabilization to the relevant transition state relative to that in the stepwise process.

It should be noted that the activation barriers obtained with the EVB method are more reliable than previous theoretical results obtained with hybrid molecular mechanical/quantum mechanical (QM/MM) methods.[29,32] The reason for this is not due to some fundamental problem in the QM/MM approach but due to the consistent calibration of the EVB method and its focus on changes in solvation energies rather than on intramolecular energies (these latter energies are similar in enzyme and solution and hence they practically cancel). Eventually, when QM/MM methods involve ab initio QM treatment and actual free-energy calculations, they will become the methods of choice.

It has been shown in this work that aldose reductase does not accelerate significantly the reduction of aldehydes relative to the reference reaction in water. This result may lead one to wonder how the enzyme can in fact catalyze the reaction if it has an activation barrier similar to that of the reference reaction in a water cage. However, our reference system corresponds to the case where the hydride- and proton-donor sites are already brought to a close proximity of the substrate. To have such a situation in a cell without the enzyme, a concentration of 55 M of both reactive groups would be required. In the case that one is interested in the rate of the reaction in water under standard conditions, a rate is obtained that is much slower than that in the enzyme. Obviously, even 1 M concentrations are not attainable for the hydride and proton donors under physiological conditions. In addition, NADPH is bound to ALR2 in an extended conformation that is unfavorable in solution but essential in the enzyme to lock the nicotinamide group of NADPH in a conformation that ensures the correct stereospecificity of the catalytic reaction. This fixed conformation in the enzyme may also reduce the entropic penalty of the association of the reactive species relative to the corresponding penalty water. At any rate, the cage concept used in the EVB approach is necessary to separate the real catalytic effect of the enzyme from the concentration effects of the cage. This approach also provides a reliable way to use solution phase experimental information about elementary steps in constructing a reference potential surface for the given enzymatic reaction.

The results of this work are consistent with the proposed evolutionary role of the enzyme in detoxification;[10,11] that is, the enzyme has evolved to recognize the carbonyl group in many structurally diverse substrates, through the essential hydrogen bonds between the carbonyl group and polar groups of Tyr-48 and His-110, and align them for the stereospecific reaction. Its large hydrophobic active site can accommodate isocorticoids,[7] but small polar substrates, such as methylglyoxal or D-glyceraldehyde, are among the "good" substrates as well.[11] The different substrates are then reduced without particular specificity at a moderate and relatively constant rate. It is probably hard for the enzyme to provide an active site that binds substrates of different sizes and polarity and subsequently catalyze their reduction beyond simply bringing the hydride and proton donor groups to the proximity of the substrate (this represents the starting point in our cage concept). This might mean that the catalytic effect which is usually provided by the preorganization of the enzyme dipoles[38] is not fully manifested here. We explain this fact with the hypothesis that the orientation of the carbonyl group in the transition state is different for different substrates (for the effect of the binding mode of a substrate on the catalytic efficiency, see a related study on Rnase A in ref 78). Hence, the enzyme could not evolve to stabilize the transition states of the catalytic reaction of rather different substrates in a much more effective way than that of water.

Although previous structural and kinetic studies contributed greatly to our present knowledge of how ALR2 works, further quantitative progress about structure function correlation can be achieved by computer simulations. In this work we have constructed energy diagrams for the catalytic reaction in a water cage which provides a reliable reference information for the energetics of alternative reaction paths in the enzyme. We used this knowledge here to quantify the catalytic mechanism in the wild-type enzyme. This reference data is also essential to determine the energetics of alternative mechanisms that are not observed experimentally but may be activated by some mutations. The evaluation of the effect of different mutations by comparing the predicted and observed effects helps in further refining our understanding of the catalytic reaction in aldose reductase and design more effective aldose reductase inhibitors.

**Acknowledgment.** A part of this work was supported by the NIH grant GM24492. P.V. is grateful for the support from the National Foundation for Cancer Research and the Overseas Research Student Awards Scheme (UK). P.V. would like to thank Professor W. G. Richards for his constant encouragement and support throughout this work.

JA994246J

(78) Glennon, T. M.; Warshel, A. *J. Am. Chem. Soc.* **1998**, *120*, 10234−10247.